ACS APPLIED MATERIALS & INTERFACES

Research Article

www.acsami.org

Preparation and Characterization of TiO_2 Barrier Layers for Dye-Sensitized Solar Cells

Yichen Zheng, Steven Klankowski, Yiqun Yang, and Jun Li*

Department of Chemistry, Kansas State University, Manhattan, Kansas 66503, United States

Supporting Information

ABSTRACT: A TiO_2 barrier layer is critical in enhancing the performance of dye-sensitized solar cells (DSSCs). Two methods to prepare the TiO_2 barrier layer on fluorine-doped tin dioxide (FTO) surface were systematically studied in order to minimize electron−hole recombination and electron backflow during photovoltaic processes of DSSCs. The film structure and materials properties were correlated with the photovoltaic characteristics and electrochemical properties. In the first approach, a porous TiO_2 layer was deposited by wet chemical treatment of the sample with $TiCl_4$ solution for time periods varying from 0 to 60 min. The N719 dye molecules were found to be able to insert into the porous barrier layers. The 20 min treatment formed a nonuniform but intact TiO_2 layer of ∼100−300 nm in thickness, which gave the highest open-circuit voltage V_{OC}, short-circuit photocurrent density J_{SC}, and energy conversion efficiency. But thicker TiO_2 barrier layers by this method caused a decrease in J_{SC}, possibly limited by lower electrical conductance. In the second approach, a compact TiO_2 barrier layer was created by sputter-coating 0−15 nm Ti metal films on FTO/glass and then oxidizing them into TiO_2 with thermal treatment at 500 °C in the air for 30 min. The dye molecules were found to only attach at the outer surface of the barrier layer and slightly increased with the layer thickness. These two kinds of barrier layer showed different characteristics and may be tailored for different DSSC studies.

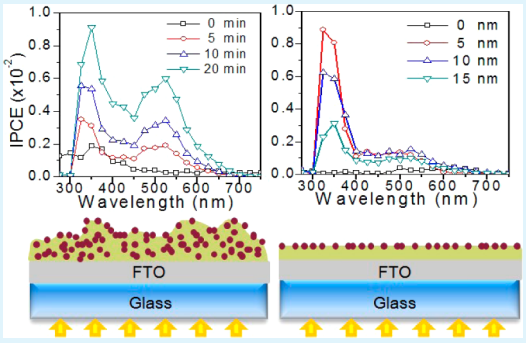

KEYWORDS: *TiO_2 barrier layer, dye sensitized solar cells, interface, photovoltaic, electron backflow*

INTRODUCTION

Dye sensitized solar cells (DSSCs)[1] have attracted great attention in recent decades because of the low cost, high sustainability, and fairly high power conversion efficiency (>10%). A high-efficient DSSC requires assembling different functional materials and optimizing their interfaces for achieving the best performance in all processes including photon capture, charge separation, electron/hole transport, and dye regeneration. One of the critical interfaces lies between the transparent conductive oxide (TCO) electrode and the mesoporous TiO_2 nanoparticle film. Studies indicated that depositing a proper TiO_2 barrier layer of tens to hundreds of nanometers between the TCO and the mesoporous TiO_2 nanoparticle film can significantly improve the solar cell efficiency.[2−10] This barrier layer helps to improve the adhesion of TiO_2 nanoparticles on the TCO surface and blocks TCO electrode from direct contact with electrolyte. It is essential in minimizing electron backflow from TCO electrode into the electrolyte and suppressing electron−hole recombination at the TCO surface. The role of the barrier layer was found increasingly important at low light intensities[9,10] and in solid-state DSSCs involving Ohmic hole-transport media.[11−13]

So far the explored methods to prepare TiO_2 barrier layer include sol−gel processes,[2,7,14] $TiCl_4$ solution treatment,[5,8,9] vacuum sputtering deposition of TiO_2,[3] and vacuum sputtering deposition of Ti metal followed by conversion into TiO_2 by acid treatment[4] or thermal oxidation.[6] The effects of the barrier layer were evaluated by comparing the performance of traditional DSSCs of ∼10 μm thick TiO_2 nanoparticle film with and without predepositing the barrier layer. In general, a compact TiO_2 layer was found to be effective in lowering the electron loss at the TCO/electrolyte interface, increasing the shunt resistance, and therefore increasing the fill factor and overall cell efficiency.[9,10] However, the function of the barrier layer was mixed with other components of the whole DSSCs and was not easily extracted from the full cell characterization. Here we report a study of DSSCs fabricated with the TiO_2 barrier layer as the sole semiconductor layer in the photoanode. The structure, photovoltaic, and electrochemical properties of the TiO_2 barrier layers prepared by two methods, i.e., $TiCl_4$ solution treatment and thermal oxidation conversion of sputter-coated Ti metal films, were systematically studied at varied thickness with and without dye sensitization. Since it avoided the overwhelming contribution from the thick mesoporous TiO_2 film, the measured photoelectron transport, back reactions, and charge recombination can be directly correlated with the materials properties of the barrier layer. This study provides a method for optimizing the TCO/TiO_2 interface in

Received: April 21, 2014
Accepted: June 13, 2014
Published: June 13, 2014

   dx.doi.org/10.1021/am502421w | ACS Appl. Mater. Interfaces 2014, 6, 10679−10686

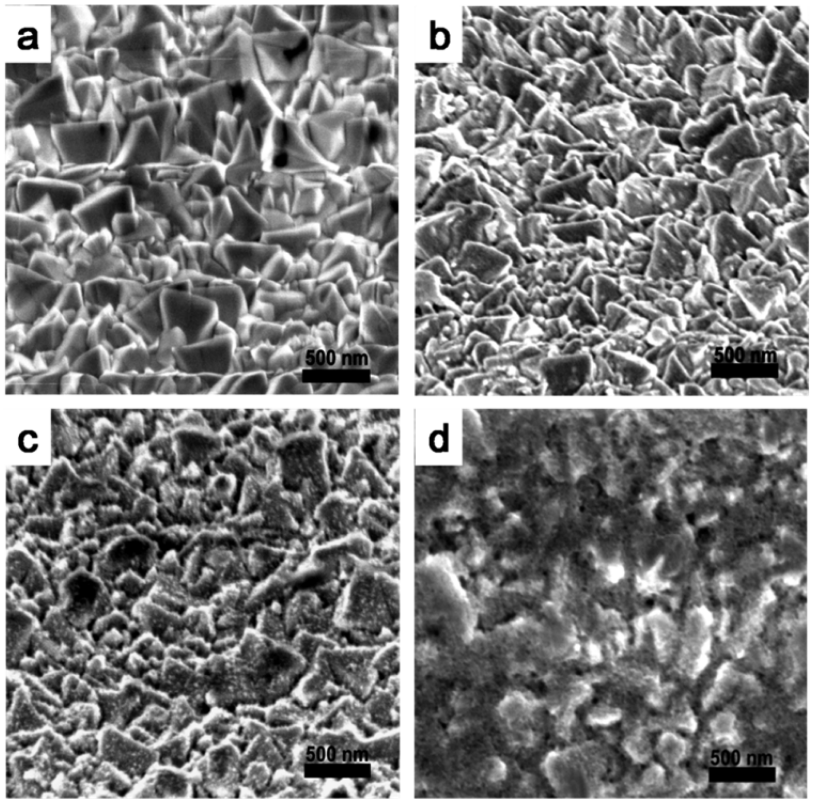

Figure 1. SEM images at 45° perspective view of (a) bare FTO/glass surface and those after (b) 20 min, (c) 40 min, and (d) 60 min $TiCl_4$ treatment.

DSSC fabrication. The thin-film DSSCs may serve as a platform for investigating photovoltaic properties of macromolecular sensitizers (such as photosynthesis complexes) that cannot easily access the interior surface of traditional mesoporous TiO_2 nanoparticle films.[15]

EXPERIMENTAL SECTION

Preparation of Photoanode of DSSC. Commercial fluorine-doped tin oxide (FTO) glass (Pilkington Glass, Lathrop, CA) was used as the photoanode substrate, which was first cleaned by sonication in isoproponal, ethanol, and acetone each for 15 min. In the second step, some FTO anodes were treated with 40 mM $TiCl_4$ solution (made by adding 99.9% $TiCl_4$ solution into deionized water) at 70 °C in oil bath with varied time from 5 to 60 min, while others were sputter-coated with a uniform Ti film at the thickness of 5, 10, and 15 nm, respectively, using a high-resolution ion beam coater (model no. 681, Gatan Inc., Pleasanton, CA). Third, after the $TiCl_4$ treatment or Ti sputtering, the photoanodes were annealed in a tube furnace open to the air at 500 °C for 30 min. This improved the crystallinity of the solution-deposited TiO_2 and converted the Ti metal into TiO_2 by thermal oxidation,[16] respectively. Finally, the annealed anodes were immersed in a 0.5 mM *cis*-diisothiocyanato-bis(2,2′-bipyridyl-4,4′-dicarboxylato)ruthenium(II) bis(tetrabutylammonium) (N-719 dye) in dried ethanol solution (Solaronix, Aubonne, Switzerland) for 12 h for dye adsorption on the TiO_2 surface. The samples were rinsed with dried ethanol to remove physisorbed dyes.

Preparation of Cathode of DSSC. Two 1 mm diameter holes were drilled at the diagonal corners of the 1 cm^2 optical window of the FTO-coated glass, and then the FTO/glass was sputtered with 25 nm thick Pt using the above ion beam coater. The Pt sputtered cathode was annealed at 450 °C in the air for activation.

Assembly and Characterization of DSSCs. The anode and cathode were bonded through a 60 μm thick hot melt spacer (Solaronix, Aubonne, Switzerland) following our previous procedure.[17] Then the Iodolyte AN-50 electrolyte (Solaronix, Aubonne, Switzerland) consisting of 50 mM triiodide, 0.1 M LiI, and 0.5 M 1,2-dimethyl-3-propylimidazolium iodide in acetonitrile filled the cell by a syringe. The assembled cell with an active area of 1 cm × 1 cm was characterized under one sun illumination with a 300 W Xe lamp solar simulator and an AM 1.5G filter (Newport, Irvine, CA) to obtain the photocurrent−voltage (I–V) curve and the dynamic responses of short-circuit current (J_{SC}) and open-circuit voltage (V_{OC}). Incident photon-to-current efficiency (IPCE) curves were measured with a 75 W Xe lamp and a monochromator (74004, Oriel Instrument, Newport, Irvine, CA).

Electrochemical and Materials Characterization. Cyclic voltammetry was carried out with a potentiostat (CHI 440A, CH Instruments, Austin, TX) in an acetonitrile solution containing 0.1 M $LiClO_4$ using a three-electrode setup vs a Pt counter electrode and a Ag/AgCl reference electrode (filled with acetonitrile solution containing 10 mM $AgNO_3$ in 1 M $LiClO_4$) to characterize the N719 dye adsorption and electrochemical activity. Scanning electron microscopy (SEM) was carried with a field-emission system (Nano430, FEI, Hillsboro, OR). Raman spectra were measured with a DXR Raman microscope (Thermo Electron, WI) using 50× objective, 530 nm laser, and 5 mW laser power.

RESULTS AND DISCUSSION

Incubating the photoanode in aqueous $TiCl_4$ solution before or after deposition of the TiO_2 nanocrystal film during DSSC fabrication has been used to form a TiO_2 thin film as the interfacial barrier layer[7,9,18] or the protecting layer.[3,13,19,20] This method was adopted as the first approach for the study of interfacial barrier layers. As shown in Figure S1 in Supporting Information, a DSSC cell with a ∼5 μm thick film formed with sintered 20 nm diameter TiO_2 nanoparticles (NPs) subjected to the $TiCl_4$ treatment both before and after TiO_2 NP film deposition shows the highest J_{SC}, largest V_{OC}, and longest electron lifetime τ_e (as indicated by the slow V_{OC} decay after

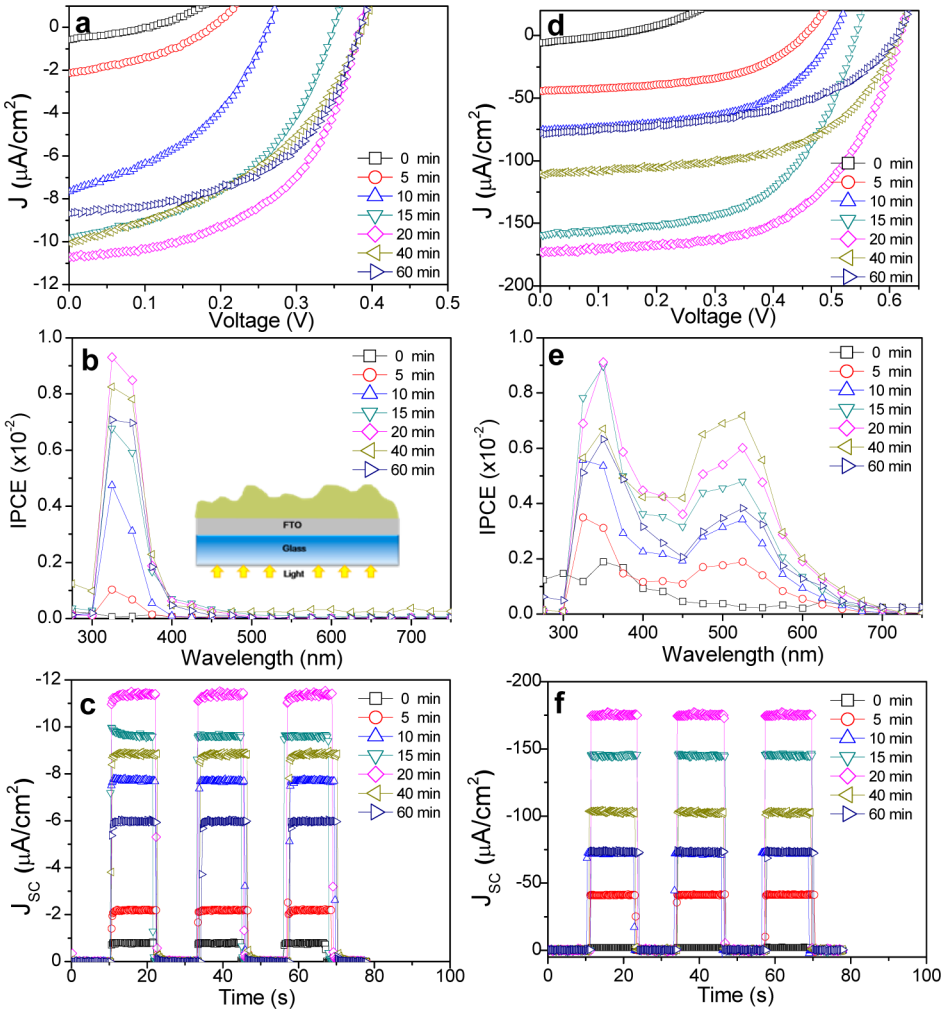

Figure 2. *I*–*V* curves (a, d), IPCE curves (b, e), and J_{SC} responses during switching light on/off (c, f) with the DSSCs made of bare FTO photoanodes and those after $TiCl_4$ treatment for 5–60 min. Panels a–c were collected with the photoanodes without N719 dye adsorption, while panels d–f were measured with samples after N719 dye adsorption.

the light was switched off[7,21]), which are consistent with literature.[7−9] The TiO_2 barrier layer is indeed critical in enhancing the DSSC performance. Since our focus here is on the understanding of the properties of TiO_2 barrier layer formed on the FTO surface, the following studies were carried out using the photoanodes with only the TiO_2 barrier layer. The thick TiO_2 NP film was skipped so that the photovoltaic information is dominated by the TCO/electrolyte interface. This is expected to show more pronounced interfacial effects similar to the studies at low light intensities.[9,10]

The SEM images in Figure 1 show the change of the top-surface morphology of the FTO/glass photoanodes as the $TiCl_4$ treatment time was increased. The starting FTO/glass sample (Figure 1a) showed typical crystalline feature of ∼200–400 nm in size. Such crystalline surface became fluffy as a thicker TiO_2 layer was deposited by increasing $TiCl_4$ treatment time. Only the samples with 20, 40, and 60 min treatment were shown because the change in the samples below 20 min of $TiCl_4$ treatment was too small to be observed. To get around with the problem of large surface roughness of the FTO electrode and estimate the deposited TiO_2 thickness, a polished Si substrate was treated with the $TiCl_4$ for 20 min following a similar procedure. Figure S2a shows the 45° perspective view SEM image, and Figure S2b shows the cross-sectional view. The TiO_2 barrier layer is not uniform, with the thickness varying from ∼100 nm in the thinnest region to ∼700 nm at thickest isolated nucleation sites, but it clearly covers the whole surface. The overall average thickness is ∼100–300 nm, comparable to the optimal thickness obtained with spray pyrolysis method on a solid-state DSSC by Peng et al.[13]

The bare FTO/glass photoanodes and those after 5–60 min of $TiCl_4$ treatment were assembled into DSSCs following the standard procedure.[1,17,22] The characteristics of these DSSCs are shown in Figure 2. To understand the origin of the photocurrent, two sets of identical samples were compared. One set was directly used without applying any dye (Figure 2a–c), and another set was incubated in a N719 solution to adsorb a monolayer of dye (Figure 2d–f). Since anatase TiO_2 is a semiconductive material with a bandgap of ∼3.2 eV, it strongly absorbs UV light with wavelength below ∼387 nm and generates a photocurrent. As a result, even the bare TiO_2/FTO/glass electrodes without dye adsorption showed clear photovoltaic properties. As the $TiCl_4$ treatment time was increased, both J_{SC} and V_{OC} increased monotonically until the maximum values were reached with the 20 min treatment. However, treatments longer than 20 min tended to reduce J_{SC} while maintaining the maximum value of V_{OC}, indicating that

the barrier layer still functioned well in blocking electron backflow but failed to collect photocurrent effectively.

The photocurrent generation by the TiO_2 layer was further illustrated in the IPCE curves in Figure 2b. Clearly, the photocurrent was completely generated by the light below ~400 nm wavelength. The IPCE value quickly increased when the wavelength was reduced below 387 nm (at which photon energy is above the bandgap of anatase TiO_2 $E_g \approx 3.2$ eV) but then sharply dropped when the wavelength was further reduced below ~320 nm (3.87 eV), forming a high IPCE band around 320−360 nm. The IPCE cutoff below ~320 nm was due to the strong absorption by the glass substrate and FTO coating (with $E_g \approx 3.6$ eV for tin oxide), which completely blocked the light from reaching the TiO_2 film. Hence the IPCE value in the 320−360 nm range represents the photovoltaic properties of the TiO_2 overlayer. Figure 2c further shows the dynamic response of J_{SC} while the photo shutter was turned on and off. When the light was turned on, the J_{SC} immediately jump to the maximum and stayed nearly constant afterward. When light was switched off, the current immediately drop to zero without any delay. The J_{SC} magnitude correlates well with the trend of $I-V$ curves vs different $TiCl_4$ treatment time in Figure 2a, which is maximum with a 20 min $TiCl_4$ treatment. The photocurrent was found to decrease as the $TiCl_4$ treatment time was increased to 40 and 60 min, presumably because electron was trapped by impurities and defects in thicker TiO_2 barrier layer as reported by Peng et al.[13]

After incubation of the TiO_2/FTO/glass in N719 solution, a monolayer of dye presumably formed on the TiO_2 surface similar to the process in general DSSC fabrication.[22] The value of J_{SC} increased by ~10−15 times as shown in Figure 2d and Figure 2f. Taking 20 min treated samples as an example, the J_{SC} is about 11 $\mu A/cm^2$ without dye (Figure 2a) but is ramped up to about 170 $\mu A/cm^2$ after dye adsorption (Figure 2d). Clearly, the dye molecule significantly enhanced the photocurrent generation. Similar to the bare TiO_2/FTO anode, both J_{SC} and V_{OC} initially increased vs the $TiCl_4$ treatment time and reached the maximum with the 20 min treatment. With longer $TiCl_4$ treatment time, the V_{OC} remained the same while the J_{SC} value decreased. It is clear that the 20 min treatment is optimum in forming an effective TiO_2 barrier layer to minimize the electron backflow to the electrolyte while suppressing its recombination with holes (oxidized dye or triiodide). However, thicker TiO_2 coating was apparently detrimental to electron transfer and adversely decreased the electron collection efficiency, leading to lower J_{SC}.

The IPCE curves in Figure 2e show a broad peak around 525 nm wavelength in addition to the TiO_2 peaks around 320−360 nm, which is attributed to the photon capture by N719 dye. The magnitude of the IPCE peak corresponding to the dye molecules is in concert with that of the TiO_2 barrier layer as the $TiCl_4$ treatment time is varied, both reaching the maximum with 20−40 min treatment. Even though the maximum IPCE value for the dye is slightly lower than that of the TiO_2 layer, it covers a broader wavelength range (from ~400 to 700 nm vs from ~300 to 400 nm) in which the standard AM1.5G solar spectrum contains a much higher number of photons N_p (see Figure S3). The photocurrent J_{SC} can be estimated by integrating (IPCE × N_p) over the wavelength range of 300−750 nm, which was indeed raised by about 10 times after N719 dye adsorption (see detailed discussions under Figure S3). The above data demonstrate that the photon absorption by thin TiO_2 layer makes only a small contribution to the overall photocurrent of the DSSC cell, but it plays an important role as a barrier layer to prevent electron backflow into the electrolyte so that a high V_{OC} can be maintained. The dye molecule makes the major contribution to the cell performance and determines the magnitude of J_{SC}, V_{OC}, and IPCE.

To further characterize the surface properties of the TiO_2 barrier layer and its effects on dye molecules adsorption, cyclic voltammetry (CV) measurements were carried out with a series of FTO/glass samples treated with $TiCl_4$ from 5 to 60 min. As shown in Figure 3a, a 20 min treated sample shows a tilt CV

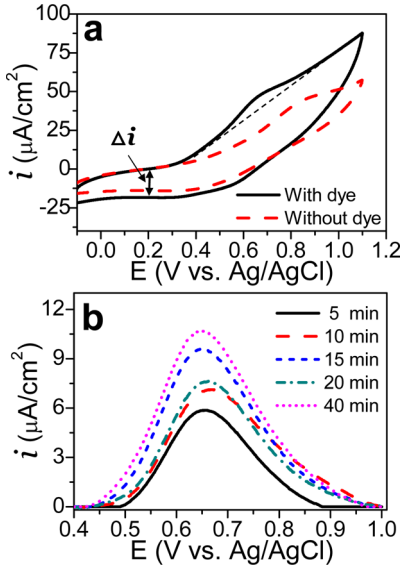

Figure 3. (a) Cyclic voltammograms of a 20 min $TiCl_4$ treated sample with and without dye adsorption. The reference electrode was Ag/AgCl in an acetonitrile filling solution containing 10 mM $AgNO_3$ in 1 M $LiClO_4$. The measurements were taken at 50 mV/s scan rate. (b) Extracted oxidation peaks of adsorbed N719 dye on FTO/glass with different $TiCl_4$ treatment time (5−60 min.), derived from the cyclic voltammograms by subtracting the linear background.

curve with a high solvent oxidation baseline above ~0.60 V vs Ag/AgCl (10 mM $AgNO_3$). After adsorption of a monolayer of N719 dye, an oxidation peak is found at ~0.65 V corresponding to oxidation of the N719 dye from Ru(II) to Ru(III). However, it does not show the corresponding reduction wave, indicating that 20 min treated TiO_2 layer serves well as a barrier to block the electron backflow. The Ru(II) oxidation peak can be extracted by subtracting a linear background (thin dashed line in Figure 3a) and is presented in Figure 3b. By dividing the integrated area A_{CV} under the subtracted CV curves with the scan rate υ, the total charge Q and subsequently the number of moles of Ru dye molecules N_{Ru} adsorbed at the surface can be derived:

$$Q = \frac{A_{CV}}{\upsilon}; \quad N_{Ru} = \frac{Q}{eF} \tag{1}$$

where e is the elementary charge. For the 20 min treated sample, the calculated total charge is 4.21×10^{-7} C/cm^2, and the adsorbed dye is 4.37×10^{-12} mol/cm^2. While the $TiCl_4$ treatment time was increased from 5 to 60 min, more dye molecules adsorbed onto the electrode surface (see Figure 3b and Figure S4).

In the meantime, the effective TiO_2 electrode surface area A_{eff} can be estimated from the separation in the baseline current of

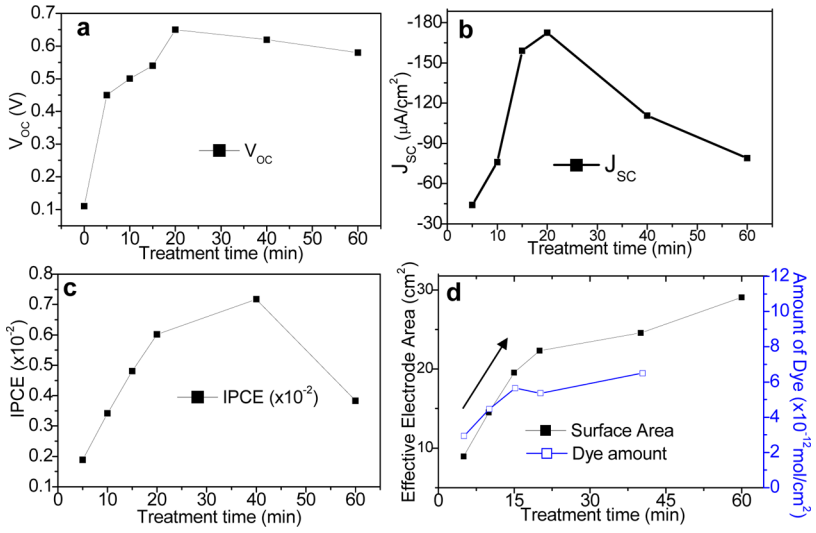

Figure 4. Comparison of (a) V_{OC}, (b) J_{SC}, (c) the maximum dye IPCE (at 525 nm), and (d) effective surface area A_{eff} on a 1 cm^2 geometric surface area and amount of dye adsorption N_{Ru} vs the $TiCl_4$ treatment time.

forward and backward scans, which is mostly attributed to the charge−discharge currents to the electrical double layer at the electrode surface. Here the current separation Δi was read at 0.20 V and A_{eff} is calculated by

$$A_{eff} = \left(\frac{\Delta i}{2}\right)/(C_0 \upsilon) \quad (2)$$

For anatase TiO_2, the specific capacitance is known to be about 90 μF/cm^2.[23] Thus, the effective surface area A_{eff} of the 20 min treated sample was calculated to be about 22.3 cm^2 on each 1.0 cm^2 geometric substrate surface area. The trend of the effective TiO_2 surface area correlates very well with that of dye adsorption vs the $TiCl_4$ treatment time.

For comparison, Figure 4 shows both of the photovoltaic properties (J_{SC}, V_{OC}, and the maximum dye IPCE) and electrochemical properties (effective TiO_2 surface area A_{eff} and amount of dye adsorption N_{Ru}). These data are quite similar to the study on barrier layer in a solid-state DSSC by Peng et al.[13] As the treatment time was raised from 0 to 20 min, A_{eff} increased linearly, leading to a proportional increase of dye adsorption as shown in Figure 4d. This indicates that the $TiCl_4$ treatment builds a porous TiO_2 barrier layer and the dye molecules can access and adsorb inside the TiO_2 layer in addition to attaching onto the outer surface. The treatments longer than 20 min, however, formed plateaus in both A_{eff} and N_{Ru} curves, indicating transforming the porous TiO_2 structure into a more compact film that only allows dye molecules to adsorb on the external surface of subsequently deposited TiO_2. The V_{OC} curve showed a very similar trend. On the other hand, IPCE and J_{SC} first increased with 0 to ~20 min $TiCl_4$ treatment time and then decreased when the time was further increased from ~20 to 60 min. It is likely that a thicker compact TiO_2 layer may hinder the electron transfer because of the low electrical conductivity.

Another piece of useful information that can be obtained regarding the barrier layer properties is the lifetime of photoexcited electrons, which can be derived from the V_{OC} decay curve after the light is switched off as shown in Figure 5. Light was first turned on for 20 s to get a stable V_{OC} and was then turned off while the V_{OC} was measured over time. Apparently the decay rates strongly depend on the TiO_2 barrier

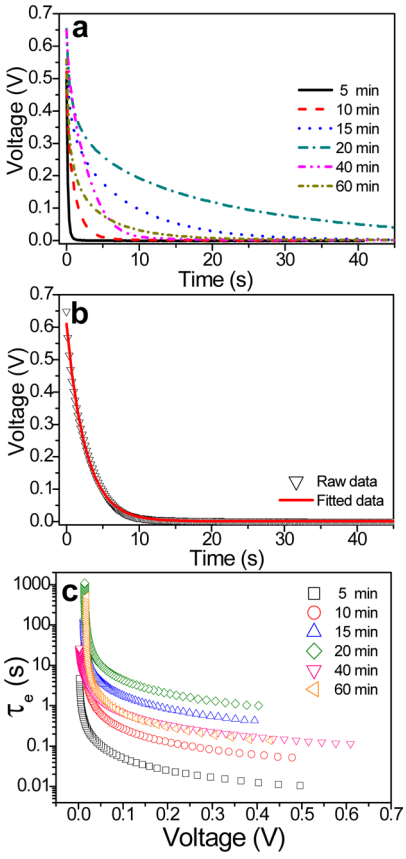

Figure 5. (a) V_{OC} decay curves of the DSSCs made of the photoanodes with different $TiCl_4$ treatment time as light was switched off. (b) Raw data and the exponential fitting of the V_{OC} decay curve of the 20 min $TiCl_4$ treated FTO/glass photoanode. (c) Comparison of the electron lifetime τ_e of different photoanodes.

layer (Figure 5a), and the decay curves can be nicely fitted with an exponential function (Figure 5b):

$$V_{OC} = A + V_{OC}^0 \, e^{-(t-t_0)/\tau} \quad (3)$$

The electron lifetime τ_e can be derived by

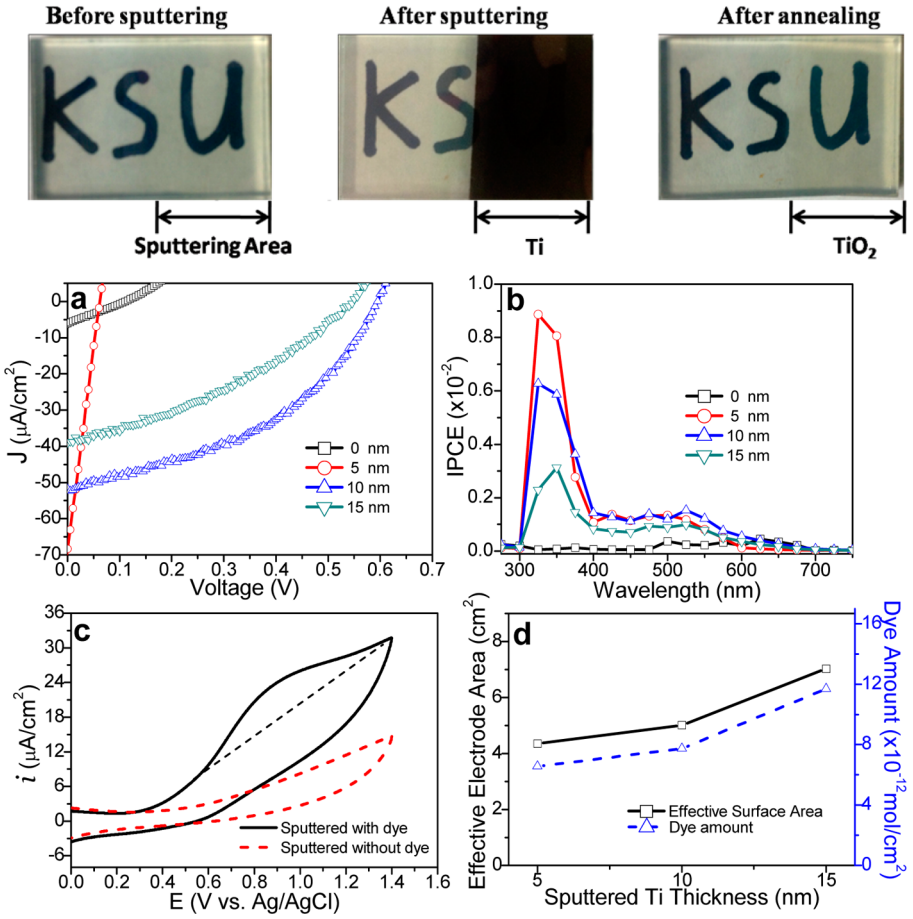

Figure 6. Top panels: Optical images of a transparent starting FTO/glass sample, after ion-sputtering with a 15 nm Ti metal film (opaque) and then further converting to TiO_2 (transparent) by thermal annealing in the air at 500 °C for 30 min. (a) $I-V$ and (b) IPCE of the DSSCs fabricated with the FTO/glass covered with the sputtering−thermal-annealing produced TiO_2 barrier layer prepared with 5, 10, and 15 nm of Ti metal film. All samples were soaked in the N719 dye solution for dye adsorption. (c) Cyclic voltammograms of a TiO_2/FTO/glass sample prepared with 10 nm sputtered Ti with and without dye adsorption. (d) Comparison of the effective electrode surface area A_{eff} on a 1 cm^2 geometric surface area and the amount of dye adsorption N_{Ru} versus the thickness of sputtered Ti film.

$$\tau_e = -(k_B T/e)(dV_{OC}/dt) \quad (4)$$

where k_B is Boltzmann constant and T is the temperature.[7,21,24] The derived τ_e is a function of V_{OC} as shown in Figure 5c. As observed, the 5 min treated sample had the smallest τ_e ranging from about ∼0.01 to ∼5 s, while the 20 min treated sample had the largest τ_e with the whole curve shifted up by nearly 2 orders of magnitude. But more than 20 min of treatment caused the curves to shift downward. The trend agrees very well with the $I-V$, IPCE, and electrochemical measurements.

Alternatively, a compact TiO_2 barrier layer can be formed by oxidation of an ion-beam sputtered Ti metal film with thermal annealing in the air at 500 °C for 30 min.[16] Compared to the nonuniform porous TiO_2 layer formed by $TiCl_4$ treatment, this sputtering−thermal-annealing method can produce much more compact and smooth TiO_2 barrier layers. The starting Ti film thickness can be precisely controlled (down to 0.1 nm) with the high-resolution ion beam coater. The top panels in Figure 6 show the conversion of an opaque Ti film into a transparent TiO_2 film by the thermal annealing process. Both $I-V$ curves (Figure 6a) and IPCE curves (Figure 6b) of the DSSCs made of N719-sensitized TiO_2/FTO/glass anodes showed strong dependence on the sputtered Ti thicknesses (5, 10, and 15 nm). Though the 5 nm sputtered sample gave the largest J_{SC}, the V_{OC} was generally very low, likely because of the incomplete TiO_2 coverage or pinholes/grain boundaries at this small thickness. Thicker TiO_2 barrier layer gave much larger and more reliable V_{OC} and decent $I-V$ curves with high fill factors. The 10 nm sputtered sample gave the best overall photovoltaic properties. Further increasing Ti sputtering to 15 nm lowered both J_{SC} and V_{OC}. The $I-V$ and IPCE of the DSSCs without dye adsorption (Figure S5) showed a similar trend. The sputtering−thermal-annealing TiO_2 barrier layer somehow affected electron transfer more than that by $TiCl_4$ treatment. In addition, compared to that of $TiCl_4$ treated sample, the IPCE value of dye molecules at ∼525 nm is much lower even though that of TiO_2 (at ∼350 nm) is comparable, indicating that the dye to TiO_2 ratio in the sputtering−thermal-annealing samples was much lower than that in $TiCl_4$ treated samples. The sputtering−thermal-annealing TiO_2 barrier layer was apparently too compact so that the dye molecules only adsorbed on the outer surface. This hypothesis was confirmed by the A_{eff} and N_{Ru} values derived from CV measurements (Figure 6c and Figure 6d) using the same method discussed earlier. As shown in Figure 6d, both of these quantities only slightly increased as the thickness of the TiO_2 barrier layer was raised (by increasing sputtered Ti thickness). The small change can be attributed to the small increase in outer surface roughness in thicker TiO_2 layers.

The structural differences of the TiO_2 barrier layers formed by $TiCl_4$ treatment and sputtering−annealing of Ti are summarized in Scheme 1. Ideally, the conformal compact barrier layer by sputtering−annealing of Ti metal would simplify the structure and thus may be a better choice. However, the chemical and materials properties of the TiO_2 film by $TiCl_4$ treatment were better for DSSCs. Particularly, 20 min $TiCl_4$ treated FTO/glass appeared to be the best TiO_2 barrier layer with ideal porosity, compactness, good electron transport, and effective backflow blocking effects. Longer $TiCl_4$ treatment tended to degrade the performance. The materials difference is further illustrated by the Raman spectra in Figure S6, which confirmed that only the $TiCl_4$ treatment produced the desired anatase TiO_2 crystal structure. A sharp peak at the Raman shift of ∼143 cm^{-1} was observed in all $TiCl_4$ treated samples with the peak intensity increasing quickly with the treatment time. In contrast, only a small anatase shoulder at ∼143 cm^{-1} and those of rutile crystal at 448 and 610 cm^{-1} were barely observed in the samples by sputtering−annealing of Ti metal. It may form amorphous or some rutile crystallites during thermal oxidation of the Ti metal at 500 °C as reported by Zhu et al.[25] This partially explains why the performance of DSSCs made with the sputtering−annealing method was worse than those by $TiCl_4$ treatments, since anatase TiO_2 is known as a better crystalline phase for DSSCs.[26]

Scheme 1. Illustration of the Differences of the TiO_2 Barrier Layers Formed by (a) $TiCl_4$ Treatment and (b) Ti Sputtering Followed by Thermal Annealing

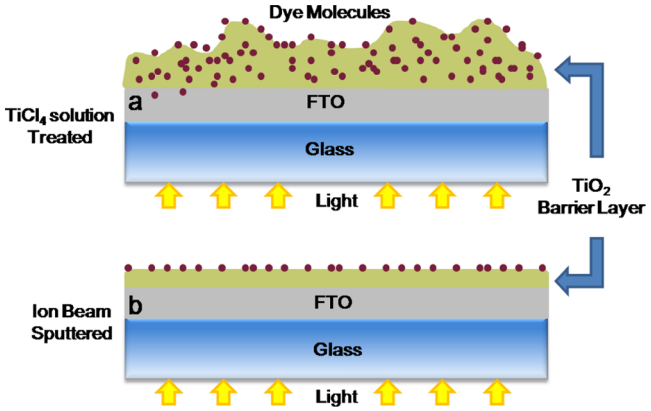

CONCLUSION

In summary, we have demonstrated two methods, the wet chemical treatment of FTO electrode with an aqueous $TiCl_4$ solution and thermal oxidation of sputter-coated Ti metal film, in preparing thin TiO_2 films as the barrier layer to prevent the photoelectron backflow from TCO to the electrolyte or electron−hole recombination at the TCO surface during DSSC operation. The structural and materials properties of the TiO_2 barrier layer were systematically characterized with electron microscopy, Raman spectroscopy, $I-V$ and IPCE measurements under light illumination, and cyclic voltammetry. The results showed consistent effects of the thickness and structure of the TiO_2 barrier layers on the DSSC performance. The proper $TiCl_4$ solution treatment produced a nonuniform porous TiO_2 film whose interior surface was accessible by the N719 dye, while the method by sputtering−annealing of Ti metal formed a smooth compact TiO_2 film with the N719 dye only adsorbed on the outer surface. Overall, the DSSCs fabricated with photoanodes by 20 min $TiCl_4$ treatment showed the best performance, likely due to the formation of desired anatase crystallites with the optimum thickness. Such thin-film DSSCs may be used as a model system to test the photovoltaic effects of new dyes or macromolecular sensitizers that cannot easily access the interior pores of traditional mesoporous DSSCs.

ASSOCIATED CONTENT

Supporting Information

$I-V$ and V_{OC} decay of traditional DSSCs with and without the TiO_2 barrier layer by $TiCl_4$ treatment, SEM characterization of TiO_2 film by $TiCl_4$ treatment on a polished Si surface, spectral irradiance and number of incident photons of 1 sun AM1.5G standard, cyclic voltammograms of the Ru(II) oxidation waves of different $TiCl_4$ treated samples, $I-V$ and IPCE of solar cells with unsensitized sputtering−annealing TiO_2 on FTO/glass, and Raman spectra of the $TiCl_4$ treated and sputtering−annealing TiO_2/FTO/glass samples. This material is available free of charge via the Internet at http://pubs.acs.org.

AUTHOR INFORMATION

Corresponding Author

*E-mail: junli@ksu.edu.

Author Contributions

The manuscript was written through contributions of all authors. All authors have given approval to the final version of the manuscript.

Notes

The authors declare no competing financial interest.

ACKNOWLEDGMENTS

This work was supported by the NSF EPSCoR Award EPS-0903806 (including the matching support from the state of Kansas through Kansas Technology Enterprise Corporation) and partially by NSF Grant CMMI-1100830 and NASA Grant NNX13AD42A.

REFERENCES

(1) O'regan, B.; Grfitzeli, M. A Low-Cost, High-Efficiency Solar Cell Based on Dye-Sensitized. *Nature* **1991**, *353*, 737−740.
(2) Hart, J. N.; Menzies, D.; Cheng, Y.-B.; Simon, G. P.; Spiccia, L. TiO_2 Sol−Gel Blocking Layers for Dye-Sensitized Solar Cells. *C. R. Chim.* **2006**, *9*, 622−626.
(3) Hattori, R.; Goto, H. Carrier Leakage Blocking Effect of High Temperature Sputtered TiO_2 Film on Dye-Sensitized Mesoporous Photoelectrode. *Thin Solid Films* **2007**, *515*, 8045−8049.
(4) Seo, H.; Son, M.-K.; Kim, J.-K.; Shin, I.; Prabakar, K.; Kim, H.-J. Method for Fabricating the Compact Layer in Dye-Sensitized Solar Sells by Titanium Sputter Deposition and Acid-Treatments. *Sol. Energy Mater. Sol. Cells* **2011**, *95*, 340−343.
(5) Shi, J.; Liang, J.; Peng, S.; Xu, W.; Pei, J.; Chen, J. Synthesis, Characterization and Electrochemical Properties of a Compact Titanium Dioxide Layer. *Solid State Sci.* **2009**, *11*, 433−438.
(6) Xia, J.; Masaki, N.; Jiang, K.; Yanagida, S. Deposition of a Thin Film of TiO_x from a Titanium Metal Target as Novel Blocking Layers at Conducting Glass/TiO_2 Interfaces in Ionic Liquid Mesoscopic TiO_2 Dye-Sensitized Solar Cells. *J. Phys. Chem. B* **2006**, *110*, 25222−25228.
(7) Yu, H.; Zhang, S.; Zhao, H.; Will, G.; Liu, P. An Efficient and Low-Cost TiO_2 Compact Layer for Performance Improvement of Dye-Sensitized Solar Cells. *Electrochim. Acta* **2009**, *54*, 1319−1324.
(8) Ito, S.; Liska, P.; Comte, P.; Charvet, R.; Pechy, P.; Bach, U.; Schmidt-Mende, L.; Zakeeruddin, S. M.; Kay, A.; Nazeeruddin, M. K.;

Gratzel, M. Control of Dark Current in Photoelectrochemical (TiO_2/I^--I^{3-}) and Dye-Sensitized Solar Cells. *Chem. Commun.* **2005**, 4351−4353.
(9) Burke, A.; Ito, S.; Snaith, H.; Bach, U.; Kwiatkowski, J.; Grätzel, M. The Function of a TiO_2 Compact Layer in Dye-Sensitized Solar Cells Incorporating "Planar" Organic Dyes. *Nano Lett.* **2008**, *8*, 977−981.
(10) Hore, S.; Kern, R. Implication of Device Functioning Due to Back Reaction of Electrons via the Conducting Glass Substrate in Dye Sensitized Solar Cells. *Appl. Phys. Lett.* **2005**, *87*, 263504.
(11) Krüger, J.; Plass, R.; Grätzel, M.; Cameron, P. J.; Peter, L. M. Charge Transport and Back Reaction in Solid-State Dye-Sensitized Solar Cells: A Study Using Intensity-Modulated Photovoltage and Photocurrent Spectroscopy. *J. Phys. Chem. B* **2003**, *107*, 7536−7539.
(12) Krüger, J.; Plass, R.; Cevey, L.; Piccirelli, M.; Grätzel, M.; Bach, U. High Efficiency Solid-State Photovoltaic Device Due to Inhibition of Interface Charge Recombination. *Appl. Phys. Lett.* **2001**, *79*, 2085−2087.
(13) Peng, B.; Jungmann, G.; Jäger, C.; Haarer, D.; Schmidt, H.-W.; Thelakkat, M. Systematic Investigation of the Role of Compact TiO_2 Layer in Solid State Dye-Sensitized TiO_2 Solar Cells. *Coord. Chem. Rev.* **2004**, *248*, 1479−1489.
(14) Ahn, K.-S.; Kang, M.-S.; Lee, J.-W.; Kang, Y. S. Effects of a Surfactant-Templated Nanoporous TiO_2 Interlayer on Dye-Sensitized Solar Cells. *J. Appl. Phys.* **2007**, *101*, 084312.
(15) Yang, Y.; Jankowiak, R.; Lin, C.; Holzwarth, A.; Li, J. Effect of the LHCII Pigment−Protein Complex Aggregation on Photovoltaic Properties of Sensitized TiO_2 Solar Cells. *Phys. Chem. Chem. Phys.*, submitted.
(16) Mor, G. K.; Shankar, K.; Paulose, M.; Varghese, O. K.; Grimes, C. A. Use of Highly-Ordered TiO_2 Nanotube Arrays in Dye-Sensitized Solar Cells. *Nano Lett.* **2006**, *6*, 215−218.
(17) Liu, J.; Kuo, Y.-T.; Klabunde, K. J.; Rochford, C.; Wu, J.; Li, J. Novel Dye-Sensitized Solar Cell Architecture Using TiO_2-Coated Vertically Aligned Carbon Nanofiber Arrays. *ACS Appl. Mater. Interfaces* **2009**, *1*, 1645−1649.
(18) Kavan, L.; Grätzel, M. Highly Efficient Semiconducting TiO_2 Photoelectrodes Prepared by Aerosol Pyrolysis. *Electrochim. Acta* **1995**, *40*, 643−652.
(19) Ahn, K.-S.; Kang, M.-S.; Lee, J.-W.; Kang, Y. S. Effects of a Surfactant-Templated Nanoporous TiO_2 Interlayer on Dye-Sensitized Solar Cells. *J. Appl. Phys.* **2007**, *101*, 084312.
(20) Hart, J. N.; Menzies, D.; Cheng, Y.-B.; Simon, G. P.; Spiccia, L. TiO_2 Sol−Gel Blocking Layers for Dye-Sensitized Solar Cells. *C. R. Chim.* **2006**, *9*, 622−626.
(21) Bisquert, J.; Fabregat-Santiago, F.; Mora-Sero, I.; Garcia-Belmonte, G.; Gimenez, S. Electron Lifetime in Dye-Sensitized Solar Cells: Theory and Interpretation of Measurements. *J. Phys. Chem. C* **2009**, *113*, 17278−17290.
(22) Vesce, L.; Riccitelli, R.; Soscia, G.; Brown, T. M.; Di Carlo, A.; Reale, A. Optimization of Nanostructured Titania Photoanodes for Dye-Sensitized Solar Cells: Study and Experimentation of $TiCl_4$ Treatment. *J. Non-Cryst. Solids* **2010**, *356*, 1958−1961.
(23) Lindstrom, H.; Sodergren, S.; Solbrand, A.; Rensmo, H.; Hjelm, J.; Hagfeldt, A.; Lindquist, S. E. Li^+ Ion Insertion in TiO_2 (Anatase). 2. Voltammetry on Nanoporous Films. *J. Phys. Chem. B* **1997**, *101*, 7717−7722.
(24) Zaban, A.; Greenshtein, M.; Bisquert, J. Determination of the Electron Lifetime in Nanocrystalline Dye Solar Cells by Open Circuit Voltage Decay Measurements. *ChemPhysChem* **2003**, *4*, 859−864.
(25) Zhu, K.; Neale, N. R.; Halverson, A. F.; Kim, J. Y.; Frank, A. J. Effects of Annealing Temperature on the Charge-Collection and Light-Harvesting Properties of TiO_2 Nanotube-Based Dye-Sensitized Solar Cells. *J. Phys. Chem. C* **2010**, *114*, 13433−13441.
(26) Zhang, J.; Li, M.; Feng, Z.; Chen, J.; Li, C. UV Raman Spectroscopic Study on TiO_2. I. Phase Transformation at the Surface and in the Bulk. *J. Phys. Chem. B* **2006**, *110*, 927−935.